Eur J Pediatr (2005) 164: 616–620
DOI 10.1007/s00431-005-1728-6

ORIGINAL PAPER

Yusuke Shiozawa · Nobutaka Kiyokawa
Masahiro Saito · Junichiro Fujimoto · Jun-ichi Hata
Yuichiro Yamashiro

Granulocytic sarcoma of the spine in a child without bone marrow involvement: a case report and literature review

Received: 8 March 2005 / Accepted: 18 May 2005 / Published online: 13 July 2005

Abstract We report a 2-year-old Japanese boy without bone marrow involvement who developed a primary granulocytic sarcoma in his spinal canal. Tumour cells were positive for myeloperoxidase, MIC2, CD56 and, CD68 on formalin-fixed, paraffin-embedded tissue sections and CD13, CD33, CD45, and CD64 on acetone-fixed fresh frozen sections. Nine months after the initiation of treatment, the tumour had significantly regressed and the patient was able to walk with help. *Conclusion*: Our patient is the youngest case of granulocytic sarcoma of the spine without bone marrow involvement. Immunohistochemical methods are very helpful in establishing a diagnosis of granulocytic sarcoma.

Keywords Granulocytic sarcoma · Myeloid sarcoma · Spinal cord compression · Without bone marrow involvement

Abbreviations AML: acute myeloid leukaemia · GS: granulocytic sarcoma

Introduction

Granulocytic sarcoma (GS), also termed extramedullary myeloid tumour, myeloid sarcoma or chloroma, is a malignant, solid tumour consisting of myeloblasts or immature myeloid cells occurring in extramedullary sites [1]. GS has often been described in association with acute myeloid leukaemia (AML), chronic myeloid leukaemia, or myeloproliferative disorders [1]; however, GS rarely presents in the absence of other haematological disease. Many of these cases are misdiagnosed as small round cell tumours such as malignant lymphoma, rhabdmyosarcoma or Ewing sarcoma [1]. GS may occur in almost any part of the body, but is most commonly seen in the skin, lymph nodes, and bone [1, 21,26]. Spinal cord compression is an uncommon symptom.

Here we report the youngest case of a primary GS occurring in the spinal canal and causing severe spinal compression in a child without bone marrow involvement. The importance of immunohistochemical studies in the diagnosis of GS without bone marrow involvement is discussed.

Y. Shiozawa · M. Saito · Y. Yamashiro
Department of Paediatrics, Juntendo University School of Medicine, Tokyo, Japan

Y. Shiozawa (✉) · N. Kiyokawa · J. Fujimoto · J. Hata
Department of Developmental Biology, National Research Institute for Child Health and Development, 2-10-1 Okura, Setagaya-ku, 154-8535 Tokyo, Japan
E-mail: y-shio@mte.biglobe.ne.jp
Tel.: +81-3-54947120
Fax: +81-3-34172496

Case report

A 2-year-old Japanese boy was taken to a local hospital complaining of external genital and lower extremity pain for a month; the patient had difficulty standing or walking. As MRI showed an epidural mass filling the spinal canal below the L3 level and extending into the left abdominal cavity (Fig. 1a, b), he was referred to our hospital for further evaluation and treatment. Although an open biopsy was planned to enable a diagnosis, his mother refused the procedure and the patient was discharged because of her decision. Three months later, however, the patient's lower extremities became paralysed and he developed bladder and bowel problems; he was thus readmitted to our hospital. On physical examination at the time of the second admission, he could not move his legs by himself and his lower extremities were more atrophic than at the previous examination. The deep tendon reflexes in his lower extremities were disturbed. A sensory assessment revealed hyperaesthesia below the level of L3. A complete blood count at the time of the second admission

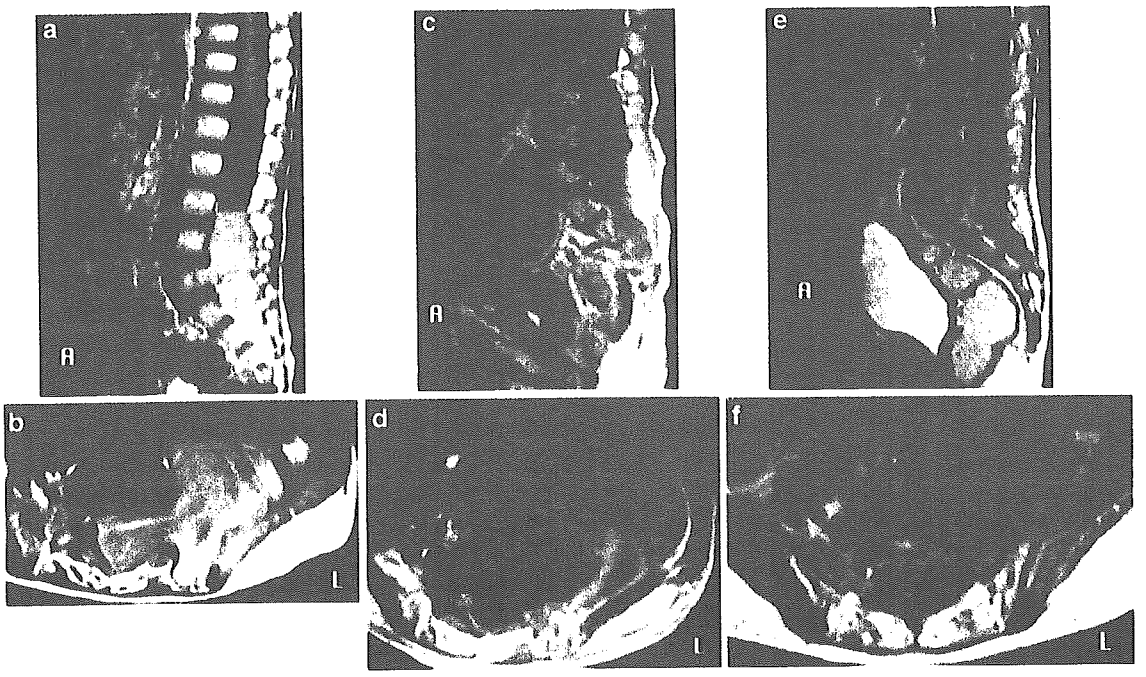

Fig. 1 a,b At the time of the initial admission, sagittal and coronal T1-weighted MRI scans showed an epidural mass filling the spinal canal below L3 and extending into the left abdominal cavity. **c,d** At the time of the second admission, the tumour had increased in size, compared to the images obtained 3 months earlier. **e,f** The size of the tumour shrunk remarkably after six courses of chemotherapy

showed a white blood cell count of 10,500 cells/μl with a normal differential, an haemoglobin level of 12.4 g/dl, and a platelet count of 289,000 cells/μl. Bone marrow aspiration showed normocellular bone marrow with no evidence of leukaemia. An MRI examination showed that the tumour had increased in size (Fig. 1c, d). An open biopsy was performed and a small round-cell-like tumour was observed in the biopsy sample. To establish a definitive diagnosis, immunohistochemical studies were performed. At this time, the tumour cells tested positive for myeloperoxidase, MIC2 (CD99), CD56, and CD68 and negative for c-Kit (CD117) and CD43 using immunohistochemical techniques on formalin-fixed, paraffin-embedded tissue sections (Fig. 2). Additional immunohistochemical studies using acetone-fixed, fresh-frozen sections revealed that the tumour cells were also positive for CD13, CD33, and CD64, all of which are markers for myeloid-lineage cells, and CD45 but negative for CD3 and CD79a (Fig. 3). Therefore, a histopathologicla diagnosis of GS was made.

First of all, we performed three courses of AML chemotherapy using etoposide, cytarabine, mitoxantron, and idarubicin (1st course: etoposide 150 mg/m^2, days 1–5, cytrabine 200 mg/m^2, days 6–12, mitoxantron 5 mg/m^2, days 6–10; 2nd course: cytarabine 3 g/m^2×2/day, days 1–3, etoposide 100 mg/m^2, days 1–5, idarubicin 10 mg/m^2, day 1; 3rd course: etoposide 150 mg/m^2, days 1–3, cytarabine 200 mg/m^2, days 4–8, mitxantron 5 mg/m^2, days 4–6). Despite this regimen, an apparent regression of the tumour was not observed. We then changed the chemotherapy to four additional courses of ifomide, pirarubicin, etoposide, and carboplatin (4th-7th course: ifomide 3 g/m^2, days 1, 2, pirarubicin 30 mg/m^2, days 4, 5, etoposide 400 mg/m^2, day 3, carboplatin 100 mg/m^2, days 1–5). In total, seven courses of chemotherapy were performed 9 months after the initiation of treatment. A subsequent MRI examination showed that the tumour had significantly regressed (Fig. 1e, f), and the patient was able to walk again with assistance.

Discussion

GS without bone marrow involvement is rare and only a few cases have presented with spinal involvement. Yamauchi et al. [26] summarised 74 GS patients without bone marrow involvement, two of their own and 72 previously reported cases; 13 out of 102 tumours (13%) in these patients had head or spinal cord involvement. Tsimberidou et al. [21] summarised GS patients without bone marrow involvement treated at the MD Anderson Cancer Center between 1990 and 2002 and reported that 4 out of 21 patients (19%) with GS without bone marrow involvement had CNS involvement. Our literature survey found only 25 GS cases without bone marrow involvement causing spinal cord compression since 1950, including the above reports (Table 1) [2, 3, 5, 7, 8, 9, 10, 11, 12, 13, 15, 16, 17, 18, 19, 20, 22, 23, 24, 25,28]. The age distribution of these patients ranged from 12 to 73 years (mean 32.2 years). Since our patient was 2 years old, he is the youngest GS patient without bone marrow involvement of the spine to be reported. 1

In our literature review including our case, the symptoms of GS causing spinal cord compression were variable depending on the patient and tumour location. Local pains were present in 88% of the patients, with

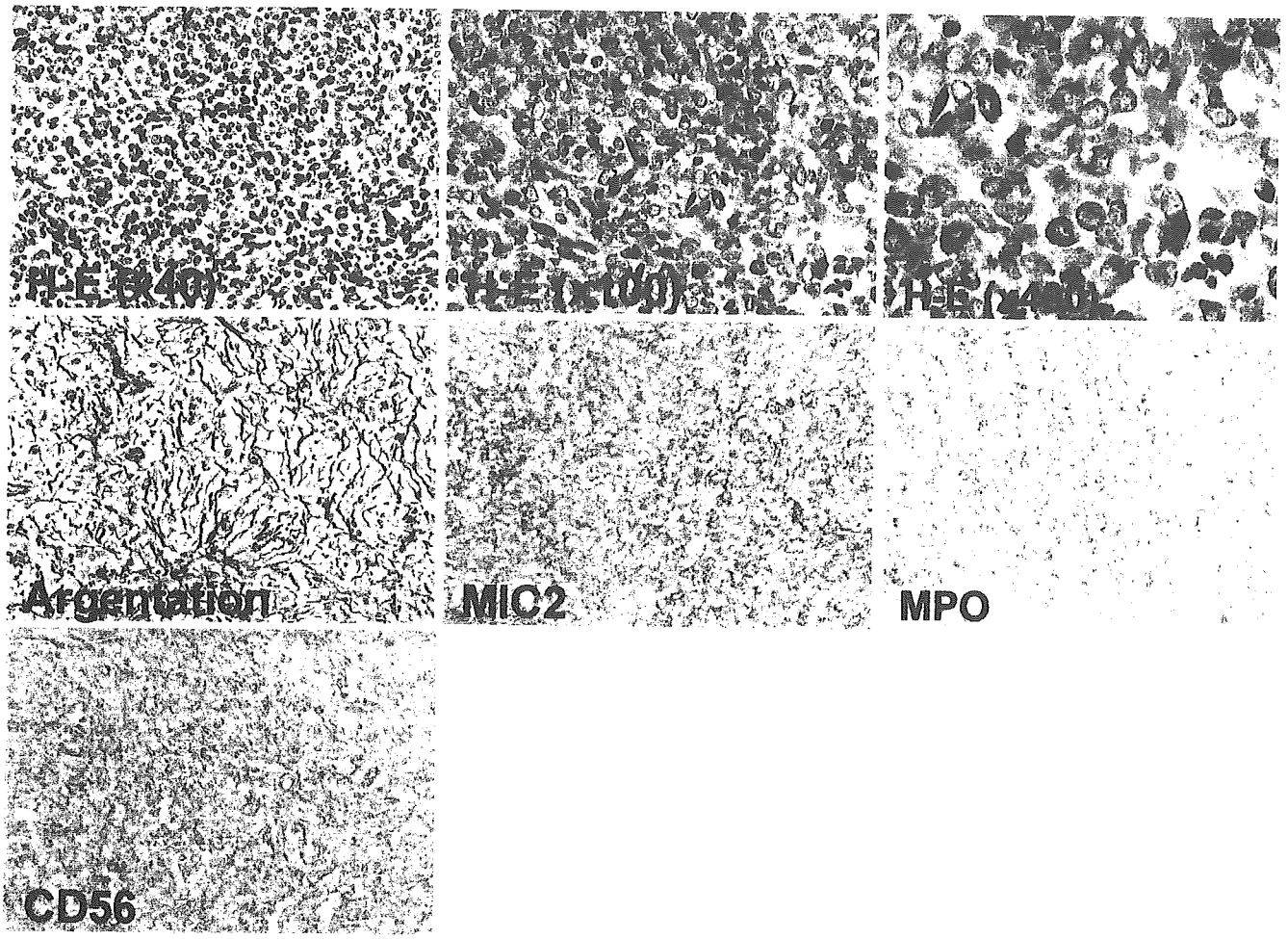

Fig. 2 Haemotoxylin and eosin and immunohistochemical staining of paraffin sections. On the stained sections, myeloid cells with round or oval nuclei, and scanty cytoplasm were generally observed. The nuclei were homogeneous, and exhibited atypia and karyomitosis. The nucleoli were obscure. On argentation, argentaffine fibres were observed twisted around the cells. On immunohistochemical-stained sections, MIC2, myeloperoxidase, CD56, and CD68 tested positive

Fig. 3 Immunohistochemical staining of acetone-fixed, fresh-frozen sections; CD13, CD33, CD45, and CD64 tested positive

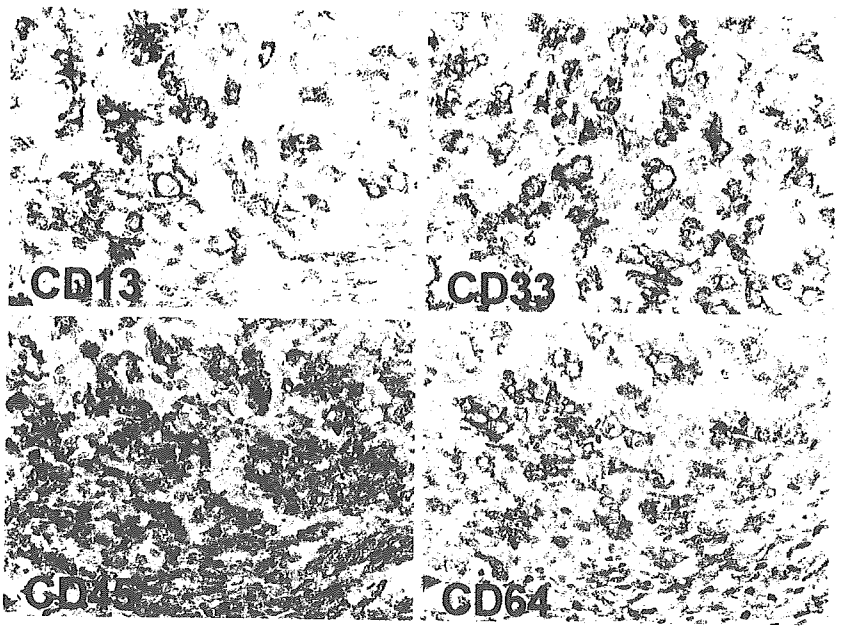

Table 1 Reported cases of GS of the spine without bone marrow involvement

No	Reference	Gender	Age (years)	Site of lesions	Treatment	Progression to leukaemia	Outcome
1	[17]	M	22	T8	Surgical decompression and radiotherapy	Negative	Death at 13 months
2	[24]	F	12	T3–T11	Surgical decompression and radiotherapy	Positive (6 months)	Death at 8 months
3	[12]	M	20	T8	Surgical decompression, radiotherapy, and chemotherapy	Positive (26 months)	Death at 43 months
4	[10]	M	33	T9–T12	Radiotherapy and chemotherapy	Negative	Survival at 14 months
5	[16]	M	21	T4–T8	Surgical decompression	Positive (29 months)	death at 29 months
6	[3]	M	13	T12–L1	Surgical decompression and radiotherapy	Negative	Survival at 72 months
7	[13]	F	29	T9–T12	Surgical decompression, radiotherapy, and chemotherapy and marrow transplantation	Positive (7 months)	Death at 1 year
8	[28]	M	31	T12–L4	Surgical decompression, radiotherapy, chemotherapy, and autologous bone marrow transplantation	Positive (32 days)	Survival at 18 months
9	[18]	M	58	T5–T8	Radiotherapy and chemotherapy	Negative	Death at 3 months
10	[8]	M	70	L2–L3	Surgical decompression, radiotherapy and chemotherapy	Negative	Survival at 3 months
11	[25]	M	49	L3–L5	Chemotherapy	Negative	Not described
12		M	36	S1	Not described	Not described	Not described
13	[23]	M	20	Less than L5	Surgical decompression, and chemotherapy	Positive (5 months)	Survival at 4 months
14	[9]	M	22	T4	Surgical decompression, radiotherapy, chemotherapy, and autologous and HLA-identical bone marrow transplantation	Positive (11 months)	Death at 29 months
15	[19]	M	22	L4–S1	Not described	Positive (4 weeks)	Not described
16	[5]	M	47	C6–C7	Surgical decompression, radiotherapy, and chemotherapy	Negative	Death at 12 months
17		M	49	L3–L4	Surgical decompression and chemotherapy	Negative	Survival at 3 months
18		M	15	L2	Surgical decompression and chemotherapy	Positive (10 months)	Death at 12 months
19	[20]	M	22	L3–S1	Radiotherapy and chemotherapy	Positive (6 weeks)	Death at 4 months
20	[15]	M	29	T2–T4	Surgical decompression, radiotherapy, and chemotherapy	Negative	Survival at 9.5 years
21	[11]	M	73	T4–T6	Surgical decompression, radiotherapy, and chemotherapy	Negative	Death at 4 months
22	[22]	M	13	T11–L1	Surgical decompression	Negative	Death at 12 months
23	[2]	F	35	C4–C5	Surgical decompression, radiotherapy, and chemotherapy	Negative	Survival at 3 months
24	[7]	M	40	S1	Surgical decompression, radiotherapy, and chemotherapy	Negative	Survival at 2 years
25		F	17	T6–T10	Chemotherapy	Negative	Survival at 2 years
26	Present case	M	2	Less than L3	Chemotherapy	Negative	Survival at 1 year

50% of these reporting back pains. Motor deficits ranging from extremity weakness to loss of bowel/bladder function (31%) or paraplegia (27%) were detected in 73% of the patients. Numbness and loss of sensation were recorded in 19% and 35% of the patients, respectively [2, 3, 5, 7, 8, 9, 10, 11, 12, 13, 15, 16, 17, 18, 19, 20, 22, 23, 24, 25,28]. If appropriate early diagnosis and early treatment are done, those symptoms can be reversible. Therefore, GS should be included in the differential diagnosis of extradural spinal cord tumours, regardless of the evidence of leukaemia.

GS is difficult to diagnose in patients without bone marrow involvement because of its rarity. Yamauchi et al. [26], Chen et al. [4], Neiman et al. [16], Eshghabadi et al. [6], and Meis et al. [13] reported that 47%, 48%, 56%, 59%, and 75% of GS patients without bone marrow involvement were initially misdiagnosed, respectively. These cases were most often misdiagnosed as lymphoproliferative disorders. In addition, small round-cell tumours, particularly in children (neuroblastoma, rhabdmyosarcoma, Ewing sarcoma/peripheral neuroectodermal tumour and medulloblastoma) must be included in the differential diagnosis [1]. Immunohistochemical methods have been reported to be helpful in establishing a diagnosis of GS [4,22]. The myelo- and/or monoblasts in GS lesions have antigenic profiles that are similar to the blasts in AML/acute monoblastic leukaemia and express myeloid- and monocytoid-associated antigens, like CD13, CD14, CD33, CD64, CD68, and c-Kit (CD117), as well as lysozyme [1]. In addition,

blasts in the GS also express leukocyte common antigen (CD45), CD43 and MIC2 (CD99). CD45 is useful for distinguishing GS from non-haematopoietic tumours but is not helpful for distinguishing GS from lymphoproliferative disorders because it is expressed in most haematopoietic tumours. CD43 is also expressed in T-cell lymphoma [14]. While MIC2 (CD99) expression has long been used as diagnostic marker for Ewing sarcoma or primitive neuroectodermal tumours; MIC2 (CD99) has also been shown to be expressed by immature myeloid cells and lymphoid cells [14,27]. C-Kit (CD117) is also highly sensitive in GS [4]. In our patient, myeloperoxidase, MIC2 (CD99), CD13, CD33, CD45, CD56, CD64, and CD68 were positive and c-Kit (CD117), CD3, CD43, and CD79a were negative. We emphasise that immunohistochemical methods are very important for the diagnosis of GS, especially the positive reaction of myeloid lineage-specific markers, such as myeloperoxidase, CD33, and CD64. Since some of these markers cannot be examined using formalin-fixed, paraffin-embedded sections, parallel examinations using acetone-fixed, fresh-frozen sections are recommended.

Although no clear relationship between specific treatment modalities and survival was found in a review of the literature [27], most GS patients without bone marrow involvement progress to AML if left untreated [5, 6,26]. In contrast, a reduced risk of developing AML was reported in GS patients without bone marrow involvement receiving chemotherapy for AML. Since early diagnosis followed by appropriate therapy may prevent leukaemic transformation in these cases, GS should be included in the differential diagnosis of extradural spinal cord tumours, regardless of the evidence of leukaemia and immunohistochemical methods are mandatory for a correct diagnosis.

References

1. Brunning RD, Matutes E, Flandrin G, Vardiman J, Bennett J, Head D, Harris NL (2001) Acute myeloid leukemia not otherwise categorised. In: Jaffe ES, Harris NL, Stein H, Vardiman JW (eds) Pathology and genetics of tumours of haematopoietic and lymphoid tissues. IARC Press, Lyon, pp 104–105
2. Buckland ME, Scolyer RA, Donellan MB, Brew S, McGee-Collett M, Harper CG (2001) Spinal chloroma presenting with triplegia in an aleukaemic patient. Pathology 33: 386–389
3. Chan JKC, Lau WH, Saw D (1986) Extradural granulocytic sarcoma of the spine: a unique case of long survival after local therapy. Am J Hematol 22: 439–441
4. Chen J, Yanuck RR, Abbondanzo SL, Chu W-S, Aguilera NSI (2001) C-Kit (CD117) reactivity in extramedullary myeloid tumor/granulocytic sarcoma. Arch Pathol Lab Med 125: 1448–1452
5. Deme S, Deodhare SS, Tucker WS, Bilbao JM (1997) Granulocytic sarcoma of spine in nonleukemic patients: report of three cases. Neurosurgery 40: 1283–1287
6. Eshghabadi M, Shajania AM, Carr I (1986) Isolated granulocytic sarcoma: report of a case and review of the literature. J Clin Oncol 4: 912–917
7. Graham A, Hodgson T, Jacubowski J, Norfolk D, Smith C (2001) MRI of perineural extramedullary granulocytic sarcoma. Neuroradiology 43: 492–495
8. Kim FSC, Rutka JT, Bernstein M, Resch L, Warner E, Pantalony D (1990) Intradural granulocytic sarcoma presenting as a lumbar radiculopathy. J Neurosurg 72: 663–667
9. Lagrange M, Gaspard M-H, Lagrange J-L, Michiels J-F, Hofman P, Thyss A, Schneider M (1992) Granulocytic sarcoma with meningeal leukemia but no bone marrow involvement at presentation. A report of two cases with characteristic cerebrospinal fluid cytology. Acta Cytol 36: 319–324
10. MaCarty KS Jr, Wortman J, Daly J, Rundles W, Hanker JS (1980) Chloroma (granulocytic sarcoma) without evidence of leukemia: facilitated light microscopic diagnosis. Blood 56: 104–108
11. Machii R, Muto A, Okano Y, Akizuki M, Katsumata Y (2000) Granulocytic sarcoma presenting as an epidural mass with spinal cord compression. Jpn J Clin Hematol 41: 653–657
12. Manson TE, Demaree RS Jr, Margolis CI (1973) Granulocytic sarcoma (chloroma), two years preceding myelogenous leukemia. Cancer 31: 423–432
13. Meis JM, Butler JJ, Osborne BM, Manning JT (1986) Granulocytic sarcoma in nonleukemic patients. Cancer 58: 2697–2709
14. Menasce LP, Banerjee SS, Beckett E, Harris M (1999) Extramedullary myeloid tumour (granulocytic sarcoma) is often misdiagdosed: a study of 26 cases. Histopathology 34: 391–398
15. Mostafavi H, Lennarson PJ, Traynelis VC (2000) Granulocytic sarcoma of the spine. Neurosurgery 46: 78–84
16. Neiman RS, Barcos M, Berard C, Bonner H, Mann R, Rydell RE, Bennett JM (1981) Granulocytic sarcoma: a clinicopathologic study of 61 biopsied cases. Cancer 48: 1426–1437
17. Ragins AB, Tinsley M (1950) Chloroma: report of a case. J Neuropathol Exp Neurol 9: 186–192
18. Ripp DJ, Davis JW, Rengachary SS, Lotuaco LG, Watanabe IS (1989) Granulocytic sarcoma presenting as an epidural mass with cord compression. Neurosurgery 24: 125–128
19. Sajjad Z, Haq N, Kandula V (1997) Case report: granulocytic sarcoma (GS) presenting as acute cord compression in a previously undiagnosed patient. Clin Radiol 52: 69–71
20. Sandhu GS, Ghufoor K, Gonzalez-Garcia J, Elexpuru-Camiruaga JA (1998) Granulocytic sarcoma presenting as cauda equina syndrome. Clin Neurol Neurosurg 100: 205–208
21. Tsimberidou A-M, Kantarjian HM, Estey E, Cortes JE, Verstovsek S, Faderl S, Thomas DA, Garcia-Manero G, Ferrajoli A, Manning JT, Keating MJ, Albitar M, O'Brien S, Giles FJ (2003) Outcome in patients with nonleukemic granulocytic sarcoma treated with chemotherapy with or without radiotherapy. Leukemia 17: 1100–1103
22. Ugras S, Cirak B, Karakok M, Guven B (2001) Spinal epidural granulocytic sarcoma (chloroma) in a non-leukemic child. Pediatr Int 43: 505–507
23. Watanabe M, Sashikata T, Kizaki T, Fujiwara T, Ugai K, Nakagawa T (1990) A case of epidural granulocytic sarcoma preceding acute leukemia. Acta Pathol Jpn 40: 922–926
24. Wilhyde DE, Jane JA, Mullan S (1963) Spinal epidural leukemia. Am J Med 34: 281–287
25. Williams M, Olliff JFC, Rowley MR (1990) CT and MR findings in parameningeal leukaemic masses. J Comput Assist Tomogr 14: 736–742
26. Yamauchi K, Yasuda M (2002) Comparison in treatments of nonleukemic granulocytic sarcoma. Cancer 94: 1739–1746
27. Zhang PJ, Barcos M, Stewart CC, Block AW, Sait S, Brools JJ (2000) Immunoreactivity of MIC2 (CD99) in acute myelogenous leukemia and related diseases. Mod Pathol 13: 452–458
28. Zuiable A, Aboud H, Nandi A, Powles R, Treleaven J (1989) Extramedullary disease initially without bone marrow involvememt in acute promyelocytic leukemia (letter). Clin Lab Haematol 2: 288–289

LIPPINCOTT WILLIAMS & WILKINS
The American Journal of Surgical Pathology

Volume 28(4), April 2004, pp 548-553

Unusual Chromaffin Cell Differentiation of a Neuroblastoma After Chemotherapy and Radiotherapy: Report of an Autopsy Case With Immunohistochemical Evaluations

[Case Report]

Miyauchi, Jun MD*; Kiyotani, Chikako MD†; Shioda, Yoko MD†; Kumagai, Masaaki MD†; Honna, Toshiro MD‡; Matsuoka, Kentaro MD*; Masaki, Hidekazu MD§; Aiba, Motohiko MD[IPN]; Hata, Jun MD¶; Tsunematsu, Yukiko MD†

From the Departments of *Clinical Laboratory, †Hematology/Oncology, ‡Surgery, and §Radiology, National Children's Hospital, Tokyo, Japan; ¶National Research Institute for Child Health and Development, Tokyo, Japan; and [IPN]Department of Pathology, Tokyo Women's Medical University Daini Hospital, Tokyo, Japan.

Reprints (present address): Jun Miyauchi, MD, Department of Clinical Laboratory, National Center for Child Health and Development, 2-10-1 Okura, Setagaya-ku, Tokyo 157-8535, Japan (e-mail: miyauchi_j@nechd.go.jp).

Abstract:

Neuroblastomas are derived from neural crest cells that are capable of multilineage differentiation. Ganglionic neuronal differentiation of childhood neuroblastoma is seen with increasing age, leading to more differentiated tumors called ganglioneuroblastomas or ganglioneuromas. Despite the fact that neuroblastomas most often arise from the adrenal medulla, chromaffin-cell differentiation in neuroblastomas is not widely recognized. Tumor cells with a chromaffin-cell nature have only been detected using histochemical techniques in neuroblastoma cell lines or focal areas of certain in vivo tumors. We describe a neuroblastoma that exhibited an unusual differentiation toward chromaffin cells in a patient that had been treated with surgery, intensive chemotherapy, and radiotherapy. Although a biopsy specimen of the retroperitoneal primary tumor was extensively necrotic, possibly because of a previous chemotherapy regimen, surgically resected metastatic tumors of bilateral ovaries were viable and diagnosed as poorly differentiated neuroblastomas according to the International Neuroblastoma Pathology Classification system. However, metastatic tumors of bilateral lungs

examined at the time of autopsy exhibited histologic features similar to those of a pheochromocytoma/paraganglioma, and immunohistochemical examinations demonstrated that these tumors were composed of extra-adrenal chromaffin cells. This case confirms that neuroblastomas in childhood can transform into pheochromocytoma/paraganglioma-like tumors under special conditions.

Neuroblastoma is the most common extracranial solid cancer that occurs during infancy and childhood.[4] Neuroblastomas are derived from embryonic neural crest cells [20] and can differentiate along the sympathetic neuronal cell pathway with increasing age. Depending on the degree of differentiation and the amount of Schwannian stromal components, neuroblastic tumors are classified into three major categories: neuroblastoma, ganglioneuroblastoma, and ganglioneuroma.[22,23] In contrast to these well-known neuronal differentiation patterns, chromaffin-cell differentiation in neuroblastomas is not widely recognized, although some investigators have histochemically demonstrated a chromaffin nature in neuroblastoma cell lines [7] as well as in focal areas of extra-adrenal tumors.[9,12,13] Despite these observations, the differentiation of neuroblastomas exclusively toward chromaffin cells is extremely rare, and only one such tumor has been previously described.[15] Here, we report a case of childhood neuroblastoma originating from the retroperitoneum with bilateral ovary metastases that were histologically diagnosed as ordinary neuroblastoma. An autopsy, performed after intensive chemotherapy and radiotherapy, revealed metastatic tumors of the lung consisting of differentiated chromaffin cells.

CASE REPORT

The patient was a 4-year-old girl who was admitted to a hospital in China complaining of abdominal distension. Histologic examinations of needle biopsy specimens from the abdominal tumor, serum analysis data (including an elevation in vanillylmandelic acid), and radiographic evaluations suggested the presence of a stage 3 neuroblastoma (International Neuroblastoma Staging System [5]). A urinary test performed in the neuroblastoma mass screening program in Japan when the patient was 6 months old had been negative. After receiving one course of chemotherapy (cyclophosphamide, 0.53 g/m^2; vincristine, 0.66 mg/m^2 ×2; THP-adriamycin, 40 mg/m^2), she was transferred to our hospital about 1 month after the onset.

A meta-iodobenzyl-guanidine scintigram revealed accumulations of radioactivity in the left renal hilus, pelvic cavity (later determined to be the left ovary), paraaortic lymph nodes, and spinal bone marrow. A computed tomographic (CT) scan revealed a retroperitoneal primary tumor and a large mass lesion in the pelvic cavity. The tumor markers were elevated as follows: neuron specific enolase = 12.3 ng/mL (normal range, <=6.0 ng/mL), vanillylmandelic acid = 255.6 μg/mg Cr (normal range, 3.5–15 μg/mg Cr), and homovanillic acid = 121.9 μg/mg Cr (normal range, 4.5–20 μg/mg Cr). Her left ovary was surgically resected because of massive enlargement, suggesting tumor metastasis, and a biopsy specimen was taken from the retroperitoneal primary tumor. The N-*myc* gene was not amplified in the resected tumor sample. After surgery, four courses of chemotherapy according to the Regimen 98A$_3$ protocol (cyclophosphamide, 1.2g/m^2 ×2; vincristine, 1.5 mg/m^2 ×1; THP-adriamycin, 40 mg/m^2 ×1; cisplatin, 25 mg/m^2 ×5 *c.i.*) of the Study Group of Japan [21] were performed, but the meta-iodobenzyl-guanidine scintigram remained positive. Following the fifth course of chemotherapy, the retroperitoneal primary tumor, the metastatic tumor in the right ovary, and the lymph nodes were surgically removed 6 months after the initial surgery. Although the values of all the

tumor markers decreased to within a normal range thereafter, the meta-iodobenzyl-guanidine scintigram still revealed an uptake of radioactivity, so an additional four courses of chemotherapy and radiation therapy were performed. The patient was scheduled to receive a bone marrow transplantation, but a chest x-ray and CT scan revealed multiple, fine, nodular lesions in bilateral lungs, and values of her tumor markers began to increase once again. After treatment with total body irradiation (12 Gy), the patient received a stem cell transplantation using umbilical cord blood, but she died of complications from the transplantation, including graft-versus-host disease and a brain hemorrhage, at the age of 5 years.

METHODS

Immunohistochemistry

An indirect immunohistochemical analysis was performed using formalin-fixed, paraffin-embedded tissue sections and the standardized streptavidin-biotin peroxidase complex method (DAKO-LSAB; Dako Japan, Kyoto, Japan) with 3,3'-diaminobenzidine as a chromogen. When required, antigen retrieval was performed according to the manufacturer's instructions. The sources and clones of the primary antibodies that were used are listed in Table 1.

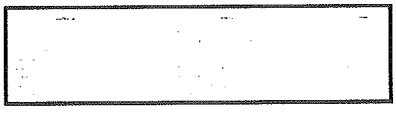

Table 1. Panel of Primary Antibodies Used in Immunohistochemistry

[Help with image viewing]
[Email Jumpstart To Image]

RESULTS

Pathologic Findings of the Surgical Materials

The left ovarian tumor, surgically resected when the patient was 4 years old, measured 12.5 × 11.5 × 8.0 cm in diameter and weighed 610 g. The cut surface of the tumor was solid, grayish brown in color, with scattered foci of necrosis. The tumor consisted of small neuroblasts with round nuclei, forming neuropils and rosettes (Fig. 1A), corresponding to a poorly differentiated neuroblastoma according to the International Neuroblastoma Pathology Classification system,[22,23] although this evaluation was made after the patient had received chemotherapy. The tumor contained thin fibrovascular stroma that partially formed a lobular architecture. The biopsy material from the retroperitoneal primary tumor, obtained simultaneously at the time of surgery, consisted of necrotic tissue with no viable tumor cells, possibly due to the chemotherapy performed in China.

FIGURE 1. Histology of the tumors. **A:** The metastatic left ovarian tumor consists of small round cells forming neuropils and rosettes, a typical histologic appearance of neuroblastoma (original magnification, ×36). **B:** The metastatic lung tumor observed at autopsy consists of compact sheets of cells with a

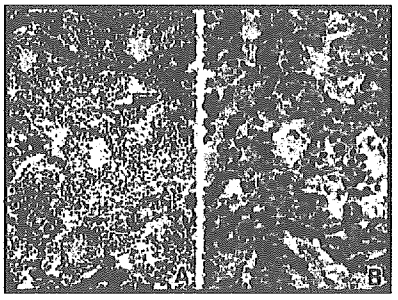

deeply basophilic cytoplasm and fibrovascular stroma, a histologic appearance similar to that of pheochromocytoma/paraganglioma (original magnification, ×60).

[Help with image viewing]
[Email Jumpstart To Image]

The right ovarian tumor, resected 6 months later, measured 4.0 × 2.7 × 2.5 cm in diameter and weighed 18 g, with its cut surface being solid and grayish brown in color. The tumor consisted of compact nests of small round neuroblasts forming neuropils, with few rosettes, and was histologically similar to the left ovarian tumor. The retroperitoneal primary tumor, resected together with the right ovary, measured 4 × 3 cm in diameter on the cut surface, exhibited extensive necrosis with calcification and hemosiderosis, and contained only tiny nests of viable neuroblastoma cells at the periphery. The left adrenal gland adjacent to the primary tumor was intact with no tumor involvement, indicating that the tumor had arisen from the retroperitoneum.

Autopsy Findings

An autopsy was performed about 8 hours after the death of the patient. Extensive dissemination of the tumor was present in bilateral lungs. The metastatic lung tumors consisted of small nodules, measuring up to 5 mm in diameter, located mainly on the pleura and in the interlobular connective tissue. The tumors were composed of solid, compact sheets of epithelial-like cells with a deeply basophilic cytoplasm and single, round to oval nuclei (Fig. 1B). The tumor stroma consisted of fine vascular channels surrounded by a small amount of fibrous tissue. These characteristics are similar to those for pheochromocytoma and paraganglioma. Neuroblasts, ganglion cells, and Schwann cells were absent. Microscopic tumor metastases were also found in the left kidney, pancreatic head, and paraaortic lymph nodes. The histologies of these metastases were basically similar to those in the lung, although degenerative changes and/or necrosis made a definite histologic diagnosis difficult.

Immunohistochemistry

Immunohistochemistry showed that the left ovarian metastatic tumor, resected during the initial surgery, was positive for Bcl-2. The tumor was also positive for chromogranin A (CGA) (Fig. 2A), synaptophysin (Syn), and CD57 (HNK-1), but only in the neuropils at the center of the rosettes. Dopamine [beta]-hydroxylase (D[beta]H), tyrosine hydroxylase (TH), and insulin-like growth factor II (IGF-II) stained weakly and/or focally positive, while phenylethanolamine N-methyltransferase (PNMT) stained negative (Table 2). These results are consistent with the characteristics of a neuroblastoma. On the other hand, the metastatic lung tumors exhibited strong and diffuse positive staining for CGA (Fig. 2B), Syn, and TH, weak to moderate positive staining for D[beta]H and IGF-II, a very weak staining reaction for CD57, and negative staining

for Bcl-2 and PNMT (Table 2). These immunohistochemical staining patterns indicated that the metastatic lung tumors were composed of chromaffin cells with an extra-adrenal phenotype. The right ovarian tumor, resected during the second surgery, exhibited positive staining for both ganglion cell and extra-adrenal chromaffin cell markers (Table 2), although the histology of the tumor resembled that of the left ovarian neuroblastoma.

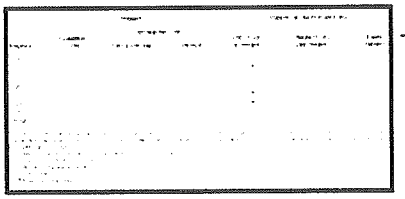

Table 2. Results of Immunohistochemistry*

[Help with image viewing]
[Email Jumpstart To Image]

FIGURE 2. Immunohistochemical staining of chromogranin A (CGA). **A:** The metastatic left ovarian tumor is positive for CGA only in the neuropils at the center of the rosettes (original magnification, ×50). **B:** The metastatic lung tumor exhibits strong, diffuse cytoplasmic staining for CGA (original magnification, ×50).

[Help with image viewing]
[Email Jumpstart To Image]

DISCUSSION

The adrenal medulla is derived from neural crest cells with a multilineage differentiation potential and is composed of heterogeneous cell types, including mostly chromaffin cells and a minor population of ganglion cells and Schwann-like supporting cells.[8,20] Reflecting this complex cellular composition, pheochromocytoma, an adrenal medullary tumor of chromaffin cells usually seen in adults, occasionally exhibits a mixed phenotype, such as pheochromocytoma admixed with ganglioneuroma, ganglioneuroblastoma, neuroblastoma, Schwannoma, or melanocytic tumors.[1-3,6,10,14,16,18,19,24] These tumors are called "composite" or "compound" tumors. On the other hand, childhood neuroblastomas are known

to differentiate along a sympathetic neuronal cell pathway with increasing age. However, the potential of neuroblastomas to differentiate along two lineages, not only neuronal cells but also chromaffin cells, has been demonstrated in neuroblastoma cell lines 7 and certain in vivo neuroblastomas 9,12,13: tumor cells with a chromaffin cell nature, detected as CGA- or IGF-II-positive cells, have been focally found in extra-adrenal neuroblastomas with a lobular architecture.12 The metastatic lung tumors in our patient arose from the extra-adrenal retroperitoneum and exhibited a lobular architecture and chromaffin cell differentiation, consistent with the above observation. Nevertheless, the conversion of a neuroblastoma to a pheochromocytoma/paraganglioma-like tumor, as seen in our case, is extremely unusual; to the best of our knowledge, a similar transformation has been described in only 1 other patient.9

Three cell types in the sympathetic neuroendocrine system, namely, adrenal and extra-adrenal chromaffin cells and sympathetic ganglion cells, can be differentiated using histochemical markers (Table 2). IGF-II is expressed in chromaffin cells but not in sympathetic neuronal cells.12,13 CGA and Syn are also useful markers of chromaffin cells, since they are strongly and diffusely expressed in chromaffin cells but only focally and weakly expressed in neuroblasts and ganglion cells.24 Bcl-2 is a marker of sympathetic neurons and is expressed in all neuroblastomas, whereas tumor cells undergoing neuroendocrine differentiation lose this antigen.11 CD57 (HNK-1) is a marker of fetal adrenal medullary ganglion cells, and its expression in neuroblastomas is uniformly associated with ganglionic differentiation but is lost with differentiation along chromaffin cell lineage.8,9,13 TH is present in all catecholamine-producing cells, while D[beta]H is expressed only in norepinephrine-producing cells and PNMT is only expressed in human adrenal medulla cells that convert norepinephrine to epinephrine.20,24 The immunohistochemical results in the present case showed that the metastatic lung tumors were of an extra-adrenal chromaffin cell lineage, although IGF-II was only weakly labeled. On the other hand, the left ovarian tumor, resected during the initial surgery, expressed antigens that were associated with ganglionic differentiation, consistent with a diagnosis of neuroblastoma. Interestingly, the histology of the right ovarian tumor, resected 6 months after the first surgery, was that of an ordinary neuroblastoma, while an immunohistochemical characterization revealed the features of both ganglionic and extra-adrenal chromaffin cells. Thus, this tumor exhibited intermediate characteristics of neuroblasts and chromaffin cells, indicating that the functional maturation of the chromaffin cells preceded any morphologic transformation.

The occurrence of an extra-adrenal pheochromocytoma as a secondary malignancy in an adolescent 15 years after the patient had been treated for a neuroblastoma has been documented.17 The pheochromocytomatous tumors in our patient, however, occurred as disseminated multiple lesions in bilateral lungs during the course of therapy, indicating that these tumors were metastatic but not a secondary malignancy. The reason why this neuroblastoma patient exhibited such an unusual differentiation pattern in her metastatic lesions, leading to a histology similar to that of a pheochromocytoma/paraganglioma, is not clear. Since the patient received intensive chemotherapy and radiotherapy, these therapies may have caused the unusual differentiation pattern by selecting special tumor clones with the capability of differentiating toward chromaffin cells. Similar phenotypic conversion has been observed in another patient 15: among the tumors that were treated with a monoclonal antibody against ganglioside G_{D2}, which is abundantly expressed on neuroblastomas, the only tumor that lost G_{D2} expression underwent pheochromocytomatous conversion, indicating a

possible association between tumor differentiation and the therapeutic treatment. The neuroblastoma in the present case was also unusual in that it metastasized to bilateral ovaries. A special genetic background may have been involved in the unique aspects of this case.

REFERENCES

1. Aiba M, Hirayama A, Ito Y, et al. A compound adrenal medullary tumor (pheochromocytoma and ganglioneuroma) and a cortical adenoma in the ipsilateral adrenal gland: a case report with enzyme histochemical and immunohistochemical studies. *Am J Surg Pathol.* 1988;12:559-566. **Bibliographic Links**| [Context Link]

2. Balazs M. Mixed pheochromocytoma and ganglioneuroma of the adrenal medulla: a case report with electron microscopic examination. *Hum Pathol.* 1988;19:1352-1355. **Bibliographic Links**| [Context Link]

3. Brady S, Lechan RM, Schwaitzberg SD, et al. Composite pheochromocytoma/ganglioneuroma of the adrenal gland associated with multiple endocrine neoplasia 2A: case report with immunohistochemical analysis. *Am J Surg Pathol.* 1997;21:102-108. **Ovid Full Text**| **Bibliographic Links**| [Context Link]

4. Brodeur GM, Castleberry RP. Neuroblastoma. In: Pizzo PA, Poplack DG, eds. *Principles and Practice of Pediatric Oncology.* 3rd ed. Philadelphia: Lippincott-Raven, 1997:761-797. [Context Link]

5. Brodeur GM, Pritchard J, Berthold F, et al. Regions of the international criteria for neuroblastoma diagnosis, staging, and response to treatment. *J Clin Oncol.* 1993;11:1466-1477. **Bibliographic Links**| [Context Link]

6. Chetty R, Clark SP, Taylor DA. Pigmented pheochromocytomas of the adrenal medulla. *Hum Pathol.* 1993;24:420-423. **Full Text**| **Bibliographic Links**| [Context Link]

7. Cooper MJ, Hutchins GM, Cohen PS, et al. Human neuroblastoma tumor cell lines correspond to the arrested differentiation of chromaffin adrenal medullary neuroblasts. *Cell Growth Differ.* 1990;1:149-159. **Bibliographic Links**| [Context Link]

8. Cooper MJ, Hutchins GM, Israel MA. Histogenesis of the human adrenal medulla: an evaluation of the ontogeny of chromaffin and nonchromaffin lineages. *Am J Pathol.* 1990;137:605-615. **Bibliographic Links**| [Context Link]

9. Cooper MJ, Steinberg SM, Chatten J, et al. Plasticity of neuroblastoma tumor cells to differentiate along a fetal adrenal ganglionic lineage predicts for improved patient survival. *J Clin Invest.* 1992;90:2402-2408. **Bibliographic Links**| [Context Link]

10. Franquemont DW, Mills SE, Lack EE. Immunohistochemical detection of neuroblastomatous foci in composite adrenal pheochromocytoma-neuroblastoma. *Am J Clin Pathol.* 1994;102:163-170. **Bibliographic Links**| [Context Link]

11. Gestblom C, Hoehner JC, Hedborg F, et al. In vivo spontaneous neuronal to neuroendocrine lineage conversion in a subset of neuroblastomas. *Am J Pathol.* 1997;150:107-117. **Bibliographic Links**| [Context Link]

12. Hedborg F, Ohlsson R, Sandstedt B, et al. IGF2 expression is a marker for paraganglionic/SIF cell differentiation in neuroblastoma. *Am J Pathol.* 1995;146:833-847. **Bibliographic Links**| [Context Link]

13. Hoehner JC, Gestblom C, Hedborg F, et al. A developmental model of neuroblastoma: differentiating stroma-poor tumors' progress along an extra-adrenal chromaffin lineage. *Lab Invest.* 1996;75:659-675. **Bibliographic Links**| [Context Link]

14. Kragel PJ, Johnston CA. Pheochromocytoma-ganglioneuroma of the adrenal. *Arch Pathol Lab Med.* 1985;109:470-472. **Bibliographic Links**| [Context Link]

15. Kramer K, Gerald WL, Kushner BH, et al. Disialoganglioside G_{D2} loss following monoclonal antibody

therapy is rare in neuroblastoma. *Clin Cancer Res.* 1998;4:2135-2139. **Bibliographic Links** | [Context Link]

16. Linnoila RI, Keiser HR, Steinberg SM, et al. Histopathology of benign versus malignant sympathoadrenal paragangliomas: clinicopathologic study of 120 cases including unusual histologic features. *Hum Pathol.* 1990;21:1168-1180. **Full Text** | **Bibliographic Links** | [Context Link]

17. López-Andreu JA, Castel V, Verdeguer A, et al. Neuroblastoma IV-S followed by extra-adrenal pheochromocytoma 15 years later. *Med Pediatr Oncol.* 1995;24:388-391. **Bibliographic Links** | [Context Link]

18. Miettinen M, Saari A. Pheochromocytoma combined with malignant schwannoma: unusual neoplasm of the adrenal medulla. *Ultrastruct Pathol.* 1988;12:513-527. **Bibliographic Links** | [Context Link]

19. Nakagawara A, Ikeda K, Tsuneyoshi M, et al. Malignant pheochromocytoma with ganglioneuroblastoma elements in a patient with von Recklinghausen' s disease. *Cancer.* 1985;55:2794-2798. **Bibliographic Links** | [Context Link]

20. Påhlman S, Hedborg F. Development of the neural crest and sympathetic nervous system. In: Brodeur GM, Sawada T, Tsuchida Y, et al, eds. *Neuroblastoma.* Tokyo: Elsevier Science, 2000:9-19. [Context Link]

21. Sawaguchi S, Kaneko M, Uchino J, et al. Treatment of advanced neuroblastoma with emphasis on intensive induction chemotherapy: a report from the Study Group of Japan. *Cancer.* 1990;66:1879-1887. **Bibliographic Links** | [Context Link]

22. Shimada H, Ambros IM, Dehner LP, et al. Terminology and morphologic criteria of neuroblastic tumors. *Cancer.* 1999;86:349-363. [Context Link]

23. Shimada H, Ambros IM, Dehner LP, et al. The international neuroblastoma pathology classification (the Shimada system). *Cancer.* 1999;86:364-372. **Full Text** | **Bibliographic Links** | [Context Link]

24. Tischler AS. Divergent differentiation in neuroendocrine tumors of the adrenal gland. *Semin Diagn Pathol.* 2000;17:120-126. **Bibliographic Links** | [Context Link]

Key Words: neuroblastoma; pheochromocytoma; paraganglioma; differentiation; chromaffin cell

---

Accession Number: 00000478-200404000-00016

Available online at www.sciencedirect.com
SCIENCE DIRECT®
Leukemia Research 29 (2005) 573–581
Leukemia Research
www.elsevier.com/locate/leukres

Dietary bioflavonoids induce apoptosis in human leukemia cells

Jun Matsui, Nobutaka Kiyokawa*, Hisami Takenouchi, Tomoko Taguchi, Kyoko Suzuki, Yusuke Shiozawa, Masahiro Saito, Wei-ran Tang, Yohko U. Katagiri, Hajime Okita, Junichiro Fujimoto

Department of Developmental Biology, National Research Institute for Child Health and Development, 2-10-1 Okura, Setagaya-ku, Tokyo 154-8535, Japan

Received 21 July 2004; accepted 11 November 2004
Available online 19 January 2005

Abstract

Dietary bioflavonoids are secondary metabolites of plants that are known to have a variety of bio-effects, including anti-cancer activity. In this study, we examined the effects of flavonoids on the growth of human leukemia cells and found that certain flavonoids induce apoptosis in a variety of human leukemia cells. The apoptosis induced by bioflavonoids was dose-dependent and was accompanied by a disruption of the mitochondrial transmembrane potential and the activation of caspase. Our data suggests that dietary bioflavonoids may be useful chemotherapeutic reagents for leukemia patients.

Keywords: Bioflavonoid; Apoptosis; Acute lymphoblastic leukemia; Precursor-B-cell

1. Introduction

Flavonoids are ubiquitously occurring and widely consumed secondary metabolites of plants [1,2]. Flavonoids can be divided into three main groups: Flavones, Flavonones (2,3-dihydroflavones), and isoflavones, which differ in structure and ring substitutions [3]. They have diverse pharmacological properties, including antioxidant, cytoprotective, and anti-inflammatory activities [1,2], and have also been reported to display anti-viral [4] and anti-parasitic [5] activities.

Moreover, some flavonoids are known to act as anti-cancer reagents. For example, Yoshida et al. reported that Quercetin markedly inhibited the growth of human gastric cancer cells [6]. Record et al. also described the inhibition of B16 melanoma cells by Genistein, both in vivo and in vitro [7]. Huang et al. demonstrated that Luteolin and Quercetin significantly inhibited the proliferation of epidermoid carcinoma A431 cells with an overexpression of epidermal growth factor receptor [8]. Indeed, some bioflavonoids like Quercetin and Genistein have already been used as chemotherapeutic agents in phase trials [9,10].

In an attempt to examine the effects of flavonoids on the growth of human leukemic cells, we challenged cultured human leukemic cell lines with several kinds of flavonoids. In the present study, we demonstrated that certain flavonoids can induce significant apoptosis in a variety of human leukemia cells.

2. Materials and methods

2.1. Cells and reagents

The cell line BV-173 that were established from a patient in an acute relapse who most likely had Ph1-positive chronic myelogenous leukemia [11]; the acute-phase of chronic myelogenous leukemia-derived cell lines K-562 (Japanese Cancer Research Resources Bank, JCRB, Tokyo, Japan)

Abbreviations: ALL, acute lymphoblastic leukemia; CD, cluster of differentiation; FITC, fluorescein isothiocyanate; PE, phycoerythrin; PC-5, PE-Cy-5; PC-7, PE-Cy-7; topo, topoisomerase

* Corresponding author. Tel.: +81 3 3417 2496; fax: +81 3 3417 2496.
E-mail address: nkiyokawa@nch.go.jp (N. Kiyokawa).

0145-2126/$ – see front matter © 2004 Elsevier Ltd. All rights reserved.
doi:10.1016/j.leukres.2004.11.015

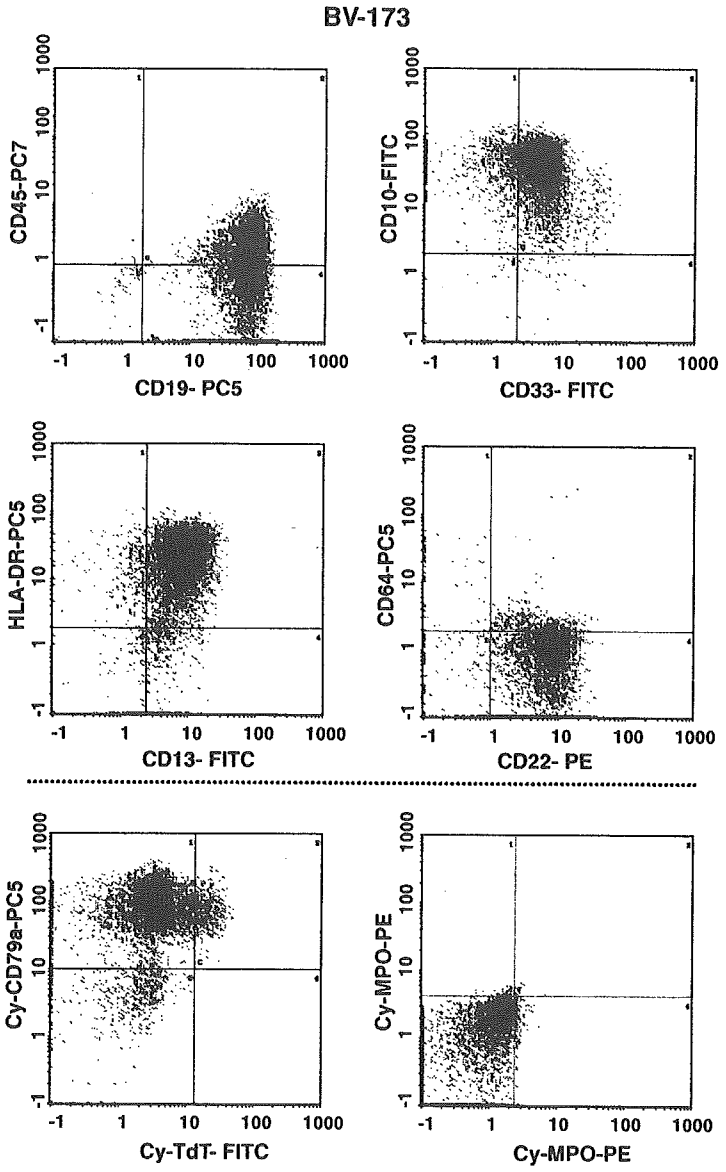

Fig. 1. Immunophenotypic analysis of BV-173 cells. The BV-173 cells were stained with fluorescence-labeled specific monoclonal antibodies against leukocyte antigens, as indicated, and analyzed by flow cytometry. The resulting histograms are shown. (Cy-) Cytoplasmic antigen stained after cell-permeabilization treatment.

and KU-812 (Institute for Fermentation, Osaka, Japan); precursor-B-acute lymphoblastic leukemia (ALL)-derived cell lines, including NALM-16, NALM-20, HPB-NULL and NALM-17 [12]; Burkitt's lymphoma-derived cell lines, Daudi and Ramos (JCRB); the histiocytic lymphoma-derived cell line U-937 (JCRB) and the acute monocytic leukemia-derived cell line THP-1 (JCRB) were used. Cells were cultured in RPMI1640 supplemented with 10% FCS at 37 °C in a humidified 5% CO_2 atmosphere.

Fluorescence-labeled monoclonal antibodies against leukocyte antigens were obtained from Beckman/Coulter Inc. (Westbrook, MA). Bioflavonoids, including Flavone, Genistein, Genistin, Quercetin, Fisetin, Luteolin, Apigenin and Rutin, and the anti-cancer drug VP-16 (which exhibits topoisomerase (topo) II-inhibitor activity) were purchased from Sigma–Aldrich (St. Louis, MO). The peptide-inhibitors for the caspases were obtained from Calbiochem-Novabiochem Co. (San Diego, CA). Bioflavonoids, VP-16 and the caspase inhibitors were desorbed in DMSO and then added to the cell cultures. All other chemical reagents were obtained from Wako Pure Chemical Industries Ltd. (Osaka, Japan), unless otherwise indicated.

2.2. *Immunofluorescence study and detection of apoptosis*

A multi-color immunofluorescence study was performed using a combination of fluorescein isothiocyanate (FITC), phycoerythrin (PE), PE-Cy-5 (PC-5) and PE-Cy-7 (PC-7). Cells were stained with fluorescence-labeled monoclonal

antibodies and analyzed by flow cytometry (EPICS-XL, Beckman/Coulter), as described previously [13]. Staining of the cytoplasmic antigens was performed using Cytofix/Cytoperm™ Kits (Becton Dickinson), according to the manufacturer's protocol.

To quantitate the incidence of apoptotic cells, cells were stained with FITC-labeled annexin V using a MEBCYTO®-Apoptosis Kit (Medical & Biological Laboratories (MBL) Co. Ltd., Nagoya, Japan) and then analyzed by flow cytometry according to the manufacturer's protocol. Experiments were performed in triplicate, and the mean ± S.D. of the cells that bound annexin V are shown. Caspase-3 activity was assessed with a PhiPhiLUX™ G1D2 kit (MBL) and analyzed by flow cytometry according to the manufacturer's protocol. The disruption of the mitochondrial transmembrane potential was detected by the MitoCapture Apoptosis Detection Kit (MBL) and analyzed by flow cytometry according to the manufacturer's protocol.

2.3. Examination of morphological appearance

BV-173 cells were immobilized onto glass slides with Cytospin 2 (Shandon Inc., Pittsburg, PA), Giemsa-stained, and their morphological appearance was examined by light microscopy (BX-61, Olympus, Tokyo, Japan).

3. Results

3.1. Immunophenotypic analysis of BV-173 cells

First, we examined the cell surface and cytoplasmic antigens expressed in BV-173 cells originally derived from a patient with Ph1-positive acute leukemia. As shown in Fig. 1, the BV-173 cells expressed B-cell antigens, such as cluster of differentiation (CD)19, CD22 and cytoplasmic CD79a, as determined by flow cytometry. Together with the expression of CD10 and HLA-DR (Fig. 1) and the absence of surface IgM (data not shown), the cell line was thought to have originated from a precursor-B-cell. However, flow cytometric analysis also revealed that the BV-173 cells simultaneously expressed myeloid antigens, including CD13 and CD33 (Fig. 1). Therefore, BV-173 was thought to exhibit biphenotypic leukemia characteristics with both precursor-B-cell and myeloid lineages. This cell line was mainly used in the following experiments.

3.2. Dietary bioflavonoids induce apoptosis in BV-173 cells

Next, we tested whether the administration of dietary bioflavonoids induced any cytotoxic effects on BV-173 cells. When BV-173 cells were treated with 200 μM of Flavone for 24 h and then examined morphologically by light microscopy, a portion of the cells exhibited condensation (arrow-head) and cleavage (arrow) of the nuclei, findings that are typical of apoptosis (Fig. 2). No such figures were observed in untreated cells (Fig. 2). The following results clearly show that the administration of Flavone indeed induced apoptosis in BV-173 cells. First, DNA prepared from BV-173 cells treated with Flavone for 24 h showed oligonucleosomal ladder fragmentation on agarose gel electrophoresis (Fig. 3). Second, the number of cells binding to annexin V increased significantly after Flavone-treatment (Fig. 4). As shown in Fig. 4, other bioflavonoids, including Luteolin, Genistein, Quercetin, and

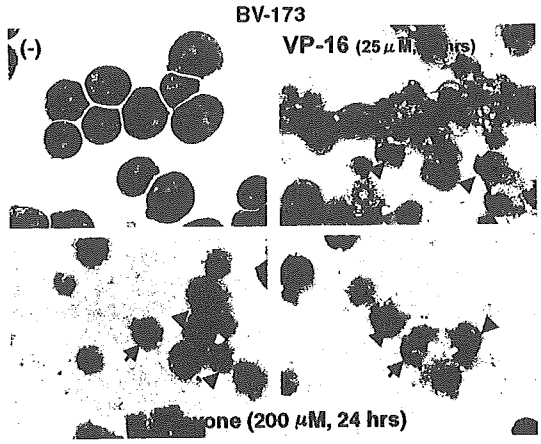

Fig. 2. Morphological examination of Flavone-treated BV-173 cells. BV-173 cells were cultured in the presence or absence of either Flavone or VP-16, as a positive control of apoptosis induction, for 24 h as indicated in the figure, then cytocentrifuged on the slide glasses. After Giemsa-staining, the morphological appearance of the cells was examined using light microscopy. The arrowheads indicate nuclear condensation. Typical apoptotic cells, characterized by cleaved nuclei, are indicated by the arrows. Magnification 400×.

Fig. 3. DNA ladder formation in BV-173 cells after Flavone-treatment. BV-173 cells were treated with (lane 4) or without (-, lane 3) 200 μM of Flavone for 24 h. The extracted DNA (1.5 μg per lane) from each sample was separated by 1% agarose gel electrophoresis. The λ/*Hin*dIII and φ/*Hae*III DNA markers were applied to the same gel (left two lanes). As a positive control for DNA ladder formation, DNA extracted from BV-173 cells treated with 25 μM of VP-16 for 24 h was also examined (VP-16, lane 5).

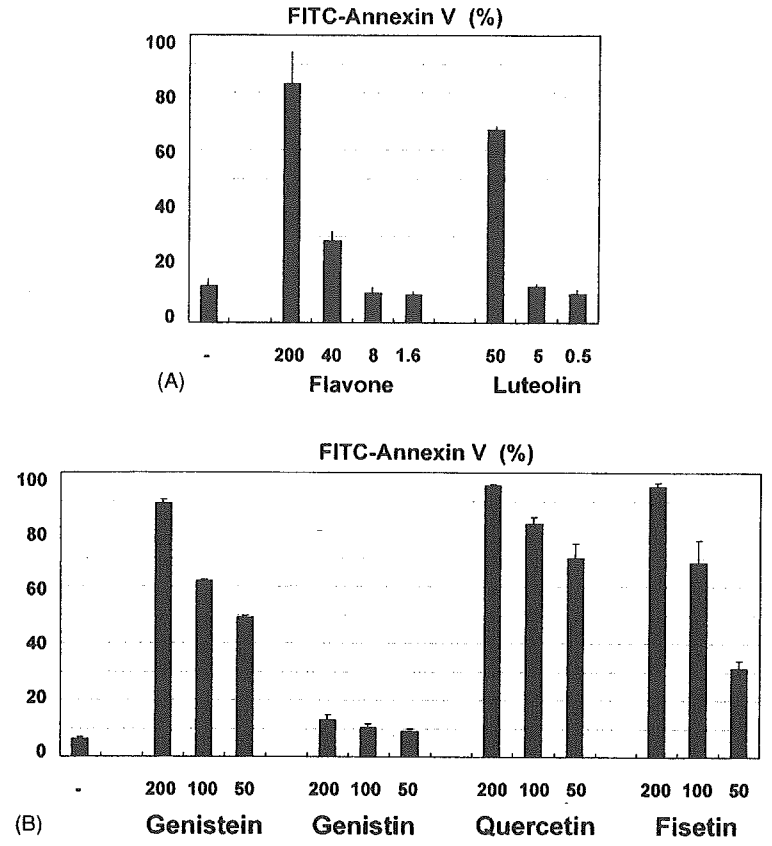

Fig. 4. Detection of annexin V binding cells after flavonoid-treatment. After culturing for 24 h in the presence of the indicated concentrations of each flavonoid, BV-173 cells were incubated with FITC-conjugated annexin V and then analyzed by flow cytometry. Experiments were performed in triplicate and the means + S.D. of the percentages of annexin V bound cells are indicated.

Fisetin, but not Genistin, also induced an increase in the number of cells binding to annexin V.

3.3. Characterization of bioflavonoid-induced apoptosis

The apoptosis induced by bioflavonoids in BV-173 cells was further characterized. In healthy cells, MitoCapture, a cationic dye, accumulates and aggregates in the mithocondria, giving off a bright red fluorescence. When the mitochondrial transmembrane potential is disrupted, however, this dye remains in the cytoplasm in its monomoer form, fluorescing green. As shown in Fig. 5, flow cytometric analysis revealed that treatment with Flavone significantly increased the number of cells with green fluorescence indicating that the mitochondrial transmembrane potential was disrupted after the induction of Flavone-induced apoptosis. In addition, Luteolin and Apigenin, but not Rutin, also disrupted the mitochondrial transmembrane potential (Fig. 5). Next, we examined the activation of caspase-3 in the process of bioflavonoid-induced apoptosis. Flow-cytometric analysis with PhiPhiLux^{TM} G1D2 indicated that treatment with Flavone significantly increased the number of cells in which caspase-3 was activated (Fig. 6). The incidence of caspase-3-activated cells induced by Flavone-treatment was much higher than that induced by VP-16-treatment (Fig. 6). Luteolin and Apigenin also increased the number of cells in which caspase-3 was activated (Fig. 6).

We further examined whether the activation of caspase was indeed involved in the bioflavonoid-induced apoptosis. As shown in Fig. 7, when BV-173 cells pretreated with either z-DEVD-fmk (a tetrapeptide inhibitor of caspase-3), z-IETD-fmk (a tetrapeptide inhibitor of caspase-8), or z-VAD-fmk (a tripeptide inhibitor of a broad range of caspases), a reduction in annexin V-positive cells after Flavone treatment was observed (Fig. 7). Of these inhibitors, z-VAD-fmk produced the most significant inhibition of Flavone-induced apoptosis in BV-173 cells.

3.4. Bioflavonoids induce apoptosis in other leukemia cell lineages

Next, we tested the effect of dietary bioflavonoids on other leukemia cell lines. As shown in Fig. 8, all of the leukemia cell lines tested in this study, including the pro-B cell lines NALM-16 and NALM-20, the pre-B cell lines HPB-NULL and NALM-17, the Burkitt's lymphoma cell lines Ramos and Daudi, the erythroleukemia cell line K-562, the basophilic leukemia cell line KU-812, the histiocytic lymphoma cell line U-937, and the acute monocytic leukemia cell line THP-1, were found to be sensitive to the apoptosis-inducing effect

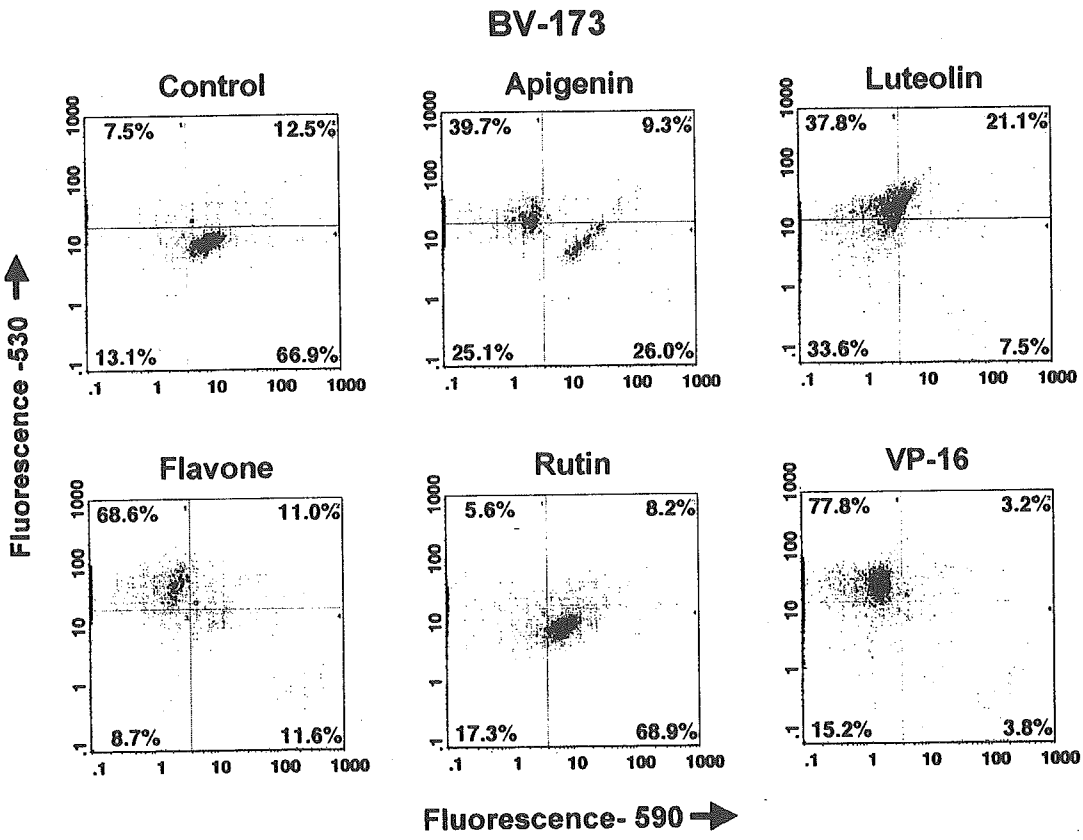

Fig. 5. Disruption of the mitochondrial transmembrane potential in BV-173 cells after bioflavonoid-treatment. BV-173 cells treated with or without flavonoids (Apigenin, 200 μM; Luteolin, 50 μM; Flavone, 200 μM; Rutin, 200 μM) or VP-16 (25 μM) for 24 h were examined using a MitoCapture Apoptosis Detection Kit and analyzed by flow cytometry. The resulting histograms are shown. *X*-axis, intensity of fluorescence -590 (red); *Y*-axis, intensity of fluorescence -530 (green). A shift in the fluorescence from red to green indicates the disruption of the mitochondrial transmembrane potential.

of dietary bioflavonoids. Among these cell lines, however, NALM-6 and K-652 exhibited a relatively lower sensitivity. Although the Burkitt's cell lines showed a limited sensitivity to VP-16 cytotoxicity, they showed a very high sensitivity to Flavone-mediated apoptosis induction.

4. Discussion

Our data clearly indicates that certain, but not all, bioflavonoids induce apoptosis in a variety of human leukemia cell types. As shown in the present study, Flavone, Luteolin, Genistein, Quercetin, and Fisetin induced significant apoptosis in BV-173 cells, while Genistin and Rutin did not. The apoptosis-inducing effect of Apigenin was intermediate. As demonstrated in the present study, all of the human leukemia cells that were tested were effectively induced to undergo apoptosis after bioflavonoid treatment. The bioflavonoid-induced apoptosis occurred in a dose-dependent manner and was accompanied by the disruption of the mitochondrial transmembrane potential and the activation of caspase-3 and perhaps caspase-8. Indeed, the apoptosis was diminished by pretreatment of the cells with anti-caspase inihibitors.

A number of studies have reported the potential ability of bioflavonoids to act as anti-cancer drugs. The precise mechanism of this phenomenon, however, remains unclear, although several effects of bioflavonoids on cell growth and cell death have been reported. For example, bioflavonoids are reported to have topo inhibitor activity. Luteolin is reported to inhibit both topo I and II and induces apoptosis in Leishmania cells [5,14]. Strick et al. [15] reported that certain bioflavonoids induce MLL gene cleavage through the inhibition of topo II.

Some topo II-inhibitors, such as VP-16 and doxorubicin, are widely used as anti-cancer reagents and have been linked with therapy-related leukemia induction due to topo II-inhibition. The effect of topo II-inhibiting substances on cells is thought to consist of two stages [16,17]. During the first stage, topo II-inhibitors stabilize topo II-cleavable complexes by forming drug:topo II:DNA ternary complexes on chromosomal DNA. This stage is reversible by DNA religation or by DNA repair. However, cellular processing of the accumulating ternary complexes triggers the initiation of apoptotic DNA cleavage, an irreversible process (secondary stage of the pathway). At this stage, it is reported that caspase-8 is activated through FADD/TRADD-dependent mechanism and plays a critical role in caspase-3 activation and apoptotic

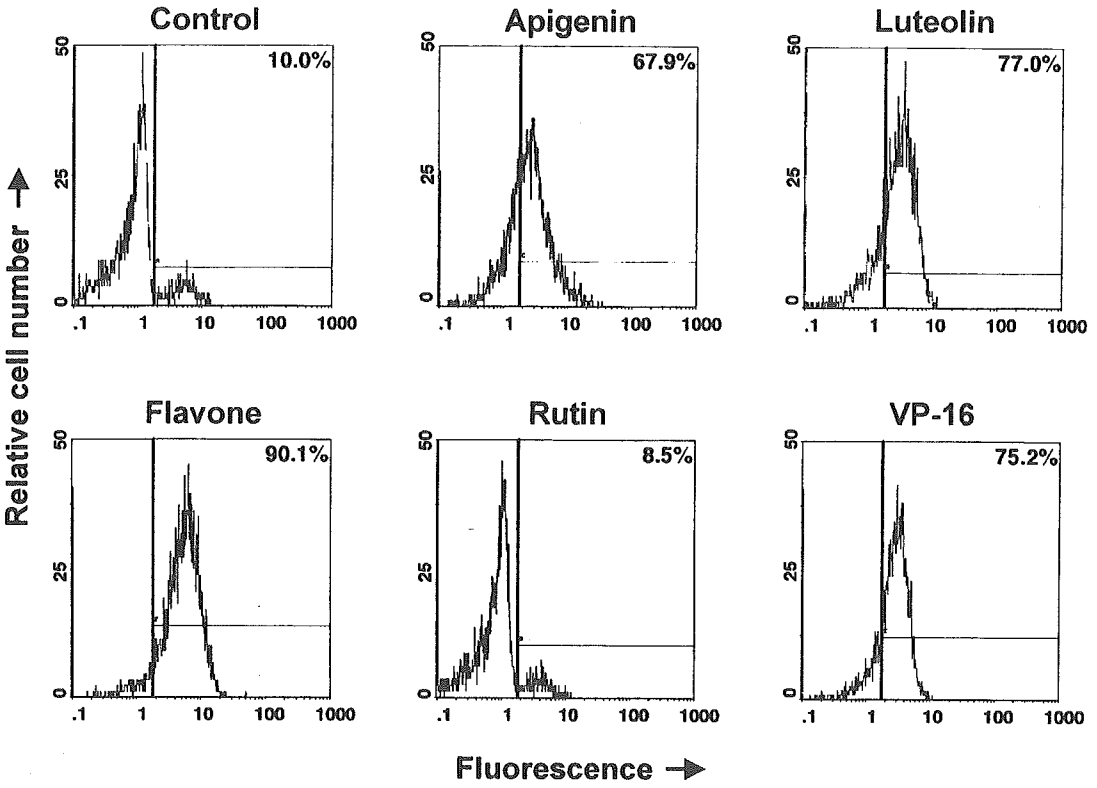

Fig. 6. Caspase-3 activity in BV-173 cells after bioflavonoid-treatment. To measure caspase-3 activity in BV-173 cells after bioflavonoid-treatment, cells prepared as in Fig. 5 were examined using PhiPhiLux^{TM} GiD2 and analyzed by flow cytometry. The resulting histograms are shown. *X*-axis, fluorescence intensity; *Y*-axis, relative cell number.

cell death [18]. In parallel, caspase-9 is also activated by apoptosome-mediated mechanism as a result of mitochondrial dysfunction. However, latter pathway seems to play a much less role in caspase-3 activation [18]. Considering the above evidence, including similar activation pattern of caspase pathway (Figs. 6 and 7), it seems reasonable to assume that the anti-cancer effect of the bioflavonoids originated in their topo II-inhibitor activity.

However, as we presented in Fig. 8, Ramos Burkitt's cells, which were resistant to VP-16, were sensitive to Flavone-induced apoptosis. In addition, Strick et al. have reported that Luteolin exhibits more strong topo II-inhibitory effect than that of Flavone [15], whereas apoptosis-inducing effect of Flavone is not lower than that of Luteolin (Fig. 8). Therefore, the induction of apoptosis by flavonoids cannot be explained solely by their topo II-inhibitory effect, and additional possible anti-cancer effects may be involved.

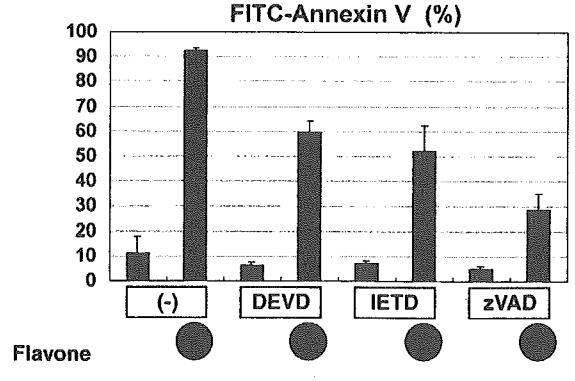

Fig. 7. Effect of caspase-inihibitors on Flavone-induced apoptosis. BV-173 cells pretreated with 50 μM of caspase-inihibitor, as indicated, were treated with 200 μM of Flavone for 24 h, as in Fig. 4. Subsequent apoptotic cells were detected by annexin V binding and analyzed by flow cytometry and are indicated as shown in Fig. 4.

Of note, K-562 cells have been reported to be topo II-resistant [19], whereas our data indicated that K-562 cells are sensitive to VP-16-induced apoptosis and show over than 70% annexin V-positive cells, similar to the flavonoids used. The precise reason for the discrepancy between the previous reports and our data is presently unclear. However, it is also reported that K-562 cells show delay in the VP-16-induced caspase activation in compared with HL-60 cells, leading to a long latent period before initiation of apoptosis, and once the active phase of apoptosis is initiated, a similar proportion of cells are ultimately killed in both cell lines [20]. Therefore, K-562 cells are not completely resistant to topo II and the sensitivity to VP-16-mediated apoptosis may vary among the stocks of K-562 cells in different laboratories.

On the other hand, some bioflavonoids, such as Genistein and Quercetin inhibited tyrosine kinase activity both in vitro and in vivo [21]. Since the overactivation of tyrosine kinases is thought to be involved in oncogenesis in many types of cancer, it seems reasonable that bioflavonoids with anti-tyrosine kinase activity would exhibit an anti-cancer effect.

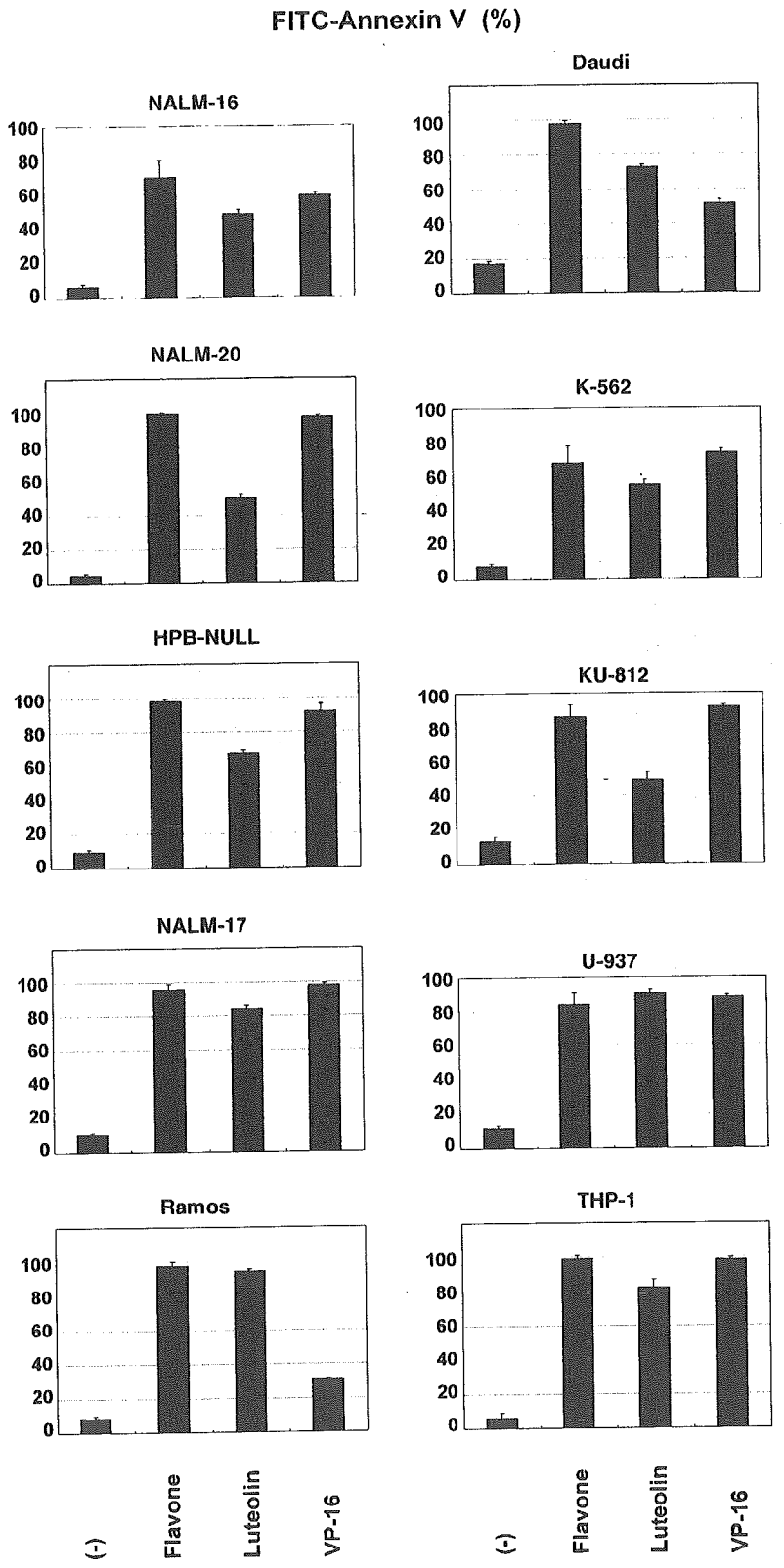

Fig. 8. Apoptosis-inducing effect of bioflavonoids in other leukemia cell lines. A variety of leukemia cell lines, as indicated in the figure, were treated with 200 μM of Flavone, 50 μM of Luteolin, or 25 μM of VP-16 (as a positive control for apoptosis induction), as in Fig. 4. Subsequent apoptotic cells were detected by annexin V binding and analyzed by flow cytometry and are indicated as shown in Fig. 4.